Tissue Architecture in the *Caenorhabditis elegans* Gonad Depends on Interactions Among Fibulin-1, Type IV Collagen and the ADAMTS Extracellular Protease

Yukihiko Kubota,*,†,1 Kayo Nagata,‡ Asako Sugimoto,† and Kiyoji Nishiwaki*,1

*Department of Bioscience, Kwansei Gakuin University, Sanda, Hyogo 669-1337, Japan, †Department of Developmental Biology and Neurosciences, Graduate School of Life Sciences, Tohoku University, Aoba-ku, Sendai 980-8577, Japan, and ‡RIKEN Center for Developmental Biology, Kobe, Hyogo 650-0047, Japan

ABSTRACT Molecules in the extracellular matrix (ECM) regulate cellular behavior in both development and pathology. Fibulin-1 is a conserved ECM protein. The *Caenorhabditis elegans* ortholog, FBL-1, regulates gonad-arm elongation and expansion by acting antagonistically to GON-1, an ADAMTS (**a** **d**isintegrin **a**nd **m**etalloprotease with **t**hrombo**s**pondin motifs) family protease. The elongation of gonad arms is directed by gonadal distal tip cells (DTCs). Here we report that a dominant mutation in the EMB-9/type IV collagen α1 subunit can compensate for loss of FBL-1 activity in gonadogenesis. A specific amino acid substitution in the noncollagenous 1 (NC1) domain of EMB-9 suppressed the *fbl-1* null mutant. FBL-1 was required to maintain wild-type EMB-9 in the basement membrane (BM), whereas mutant EMB-9 was retained in the absence of FBL-1. EMB-9 (either wild type or mutant) localization in the BM enhanced PAT-3/β-integrin expression in DTCs. In addition, overexpression of PAT-3 partially rescued the DTC migration defects in *fbl-1* mutants, suggesting that EMB-9 acts in part through PAT-3 to control DTC migration. In contrast to the suppression of *fbl-1(tk45)*, mutant EMB-9 enhanced the gonadal defects of *gon-1(e1254)*, suggesting that it gained a function similar to that of wild-type FBL-1, which promotes DTC migration by inhibiting GON-1. We propose that FBL-1 and GON-1 control EMB-9 accumulation in the BM and promote PAT-3 expression to control DTC migration.

COLLECTIVE cell migration is among the major strategies to shape tissues and organs (Bianco *et al.* 2007; Ewald *et al.* 2008; Lu and Werb 2008; Montell 2008; Friedl and Gilmour 2009; Rorth 2009). In this process, remodeling of the extracellular matrix (ECM) positively and negatively affects the interactions between basement membranes (BMs) and migrating cells or epithelia to yield the proper cell geometry and tissue architecture. However, how the ECM is remodeled and how migrating cells interact with changing ECM milieus during organogenesis is mostly unknown.

The development of *Caenorhabditis elegans* hermaphrodite gonads is regulated by migration of the gonadal leader cells, distal tip cells (DTCs), which promote the directional elongation of the gonad arms during the larval stages to form the U-shaped gonads found in adult animals (Kimble and Hirsh 1979; Hedgecock *et al.* 1987). Two secreted ADAMTS family metalloproteases, GON-1 and MIG-17, act cooperatively in this process; GON-1 is required for the motility of DTCs and gonadal expansion, whereas MIG-17 acts to control the direction of DTC movement but does not control DTC motility *per se* (Blelloch and Kimble 1999; Nishiwaki *et al.* 2000). GON-1 expressed in DTCs and that expressed in body wall muscles regulate gonadal elongation and expansion, respectively (Blelloch and Kimble 1999). GON-1 and MIG-17 are proposed to remodel the BM proteolytically to regulate the microenvironment that affects gonad shaping (Blelloch *et al.* 1999; Blelloch and Kimble 1999; Nishiwaki *et al.* 2000). GON-1 and FBL-1, a fibulin-1 ortholog in *C. elegans*, act antagonistically during gonadogenesis (Hesselson *et al.* 2004). GON-1 is homologous to mammalian ADAMTS (**a** **d**isintegrin **a**nd **m**etalloprotease

doi: 10.1534/genetics.111.133173
Manuscript received July 23, 2011; accepted for publication January 11, 2012
Supporting information is available online at http://www.genetics.org/content/suppl/2012/01/31/genetics.111.133173.DC1.
[1]Corresponding authors: Department of Developmental Biology and Neurosciences, Graduate School of Life Sciences, Tohoku University, 2-1-1 Katahira, Aoba-ku, Sendai 980-8577, Japan. E-mail: yu-kubota@m.tohoku.ac.jp and nishiwaki@kwansei.ac.jp

with thrombospondin motifs) proteinases ADAMTS-9 and ADAMTS-20 (Llamazares *et al.* 2003; Somerville *et al.* 2003). ADAMTS-5, ADAMTS-9, and ADAMTS-20 cooperate with fibulin-1 to promote regression of the interdigital web by generating active versican fragments in the mouse (McCulloch *et al.* 2009).

To uncover new components involved in the antagonistic interaction between FBL-1 and GON-1 to control gonadogenesis, we conducted a suppressor analysis of *fbl-1(tk45)* null mutants. Two independently isolated suppressors were found to be identical mutations in the gene *emb-9*, which was previously identified by embryonic lethal mutations and encodes the type IV collagen α1 chain (Miwa *et al.* 1980; Guo *et al.* 1991). In contrast to the suppression of *fbl-1*, the *emb-9* mutation enhanced the gonadal defects of *gon-1*. We also found that the reduced expression of PAT-3/β-integrin in DTCs of *fbl-1* mutants was restored to the wild-type levels in the suppressor *emb-9* mutant background. Our findings suggest that intermolecular interactions among FBL-1, EMB-9, and GON-1 regulate the type IV collagen-dependent extracellular microenvironment that involves the activation of integrin-mediated organogenesis.

Materials and Methods

Strains and genetic analysis

Culture, handling, and ethyl methanesulfonate (EMS) mutagenesis of *C. elegans* were conducted as described (Brenner 1974). Worms were grown at 20° unless otherwise noted. The following mutations and genetic balancers were used in this work: *emb-9(g34, g23cg46, tk75)*, *fbl-1(tk45)*, *gon-1(e1254, q518)*, *unc-119(e2498)*, *hT2[bli-4(e937) let-?(q782) qIs48]*, and *nT1[qIs51]* (Gupta *et al.* 1997; Blelloch and Kimble 1999; Nishiwaki *et al.* 2000; Kubota *et al.* 2004; Hesselson and Kimble 2006). *rhIs2[pat-3::GFP]* is a genomic insertion of functional *pat-3::GFP* genes (Plenefisch *et al.* 2000). For suppressor screening, *fbl-1(tk45)*; *Ex[fbl-1(+), sur-5::GFP]* hermaphrodites were used for EMS mutagenesis. The suppressor mutants *tk75* and *tk76* were isolated as described (Kubota *et al.* 2004) and backcrossed four times. The dominancy of the *emb-9(tk75)* mutation on *fbl-1* phenotypes was examined as follows: *unc-119(e2498)*; *fbl-1(tk45)/nT1[qIs51]* hermaphrodites were mated with *emb-9(tk75)*; *fbl-1(tk45)* males, and gonadal phenotypes of non-uncoordinated hermaphroditic progeny without GFP were scored. Gene dosage effects of the *emb-9* mutation on *fbl-1* phenotypes were examined as follows: *unc-119(e2498)*; *fbl-1(tk45)/nT1[qIs51]* hermaphrodites were mated with *emb-9(g23cg46)/hT2[bli-4(e937) let-?(q782) qIs48]*; *fbl-1(tk45)*; *Ex[fbl-1(+), sur5::GFP]* males, and gonadal phenotypes of non-uncoordinated hermaphroditic progeny without GFP were scored. The dominancy of the *emb-9(tk75)* mutation on *gon-1* phenotypes was examined as follows: *unc-119(e2498)*; *gon-1(e1254)/nT1[qIs51]* hermaphrodites were mated with *emb-9(tk75)*; *gon-1(e1254)/nT1[qIs51]* males, and gonadal phenotypes of non-uncoordinated hermaphroditic progeny without GFP were scored. Gene dosage effects of the *emb-9* mutation on *gon-1(e1254)* phenotypes were examined as follows: *unc-119(e2498)*; *gon-1(e1254)/nT1[qIs51]* hermaphrodites were mated with *emb-9(g23cg46)/hT2[bli-4(e937) let-?(q782) qIs48]*; *gon-1(e1254)*; *Ex[gon-1(+), sur-5::GFP]* or *emb-9(tk75)*; *gon-1(e1254)/nT1[qIs51]* males, and gonadal phenotypes of non-uncoordinated hermaphroditic progeny without GFP were scored.

Microscopy

Gonad migration phenotypes were scored using a Nomarski microscope (Axioplan 2; Zeiss). Analysis of gonadal phenotypes was performed at the young-adult stage as described (Nishiwaki 1999). A germline leakage phenotype was observed in 1-day-old adults. The localization of EMB-9, NID-1, and PAT-3–GFP was analyzed using a confocal laser scanning microscope (LSM5; Zeiss) equipped with a C-apochromat ×63 (water immersion; NA 1.2) lens and controlled by PASCAL version 3.2 SP2 software. Fluorescence microscopy was performed using the Axioplan 2 microscope. Images were captured with a Hamamatsu Photonics Chilled 3-CCD camera C5810 connected to a Windows computer (Dell).

Molecular cloning of suppressors

Single-nucleotide polymorphism (SNP) mapping (Wicks *et al.* 2001) and genomic sequence analysis of *tk75* identified a point mutation from GGA to GAA (G1708E) in *emb-9A*. The PCR-amplified *emb-9* fragment from *emb-9(tk75)*; *fbl-1(tk45)* rescued the gonadal elongation defect and sterility of *fbl-1(tk45)* mutants. *tk76* was identical to the *emb-9(tk75)* mutation.

Constructs

The wild-type *emb-9*, which corresponds to nucleotide positions 11,047–499 of the cosmid K04H4, was subcloned into PBSII KS(−). The *emb-9(tk75)* gene was constructed by introducing the *tk75* mutation into the wild-type construct by site-directed mutagenesis.

Germline transformation

Germline transformation was carried out as described (Mello *et al.* 1991). Wild-type and mutant *emb-9* plasmids were injected at 5 ng/μl with 55 ng/μl pBluescript KS(−) (carrier DNA), 20 ng/μl *unc-119*$^{+}$ plasmid (pDP#MM016B) (Maduro and Pilgrim 1995), and 70 ng/μl marker plasmid (*sur-5::GFP*) (Yochem *et al.* 1998).

Antibody staining

Preparation of frozen sections and antibody staining were as described (Kubota *et al.* 2006). The primary antibodies were anti–EMB-9 (NW1910; 1:200) (Graham *et al.* 1997) and anti–NID-1 (5 μg/ml) (Kubota *et al.* 2008); Alexa Fluor 594-conjugated goat antirabbit IgG (1:500; Molecular Probes) was the secondary antibody.

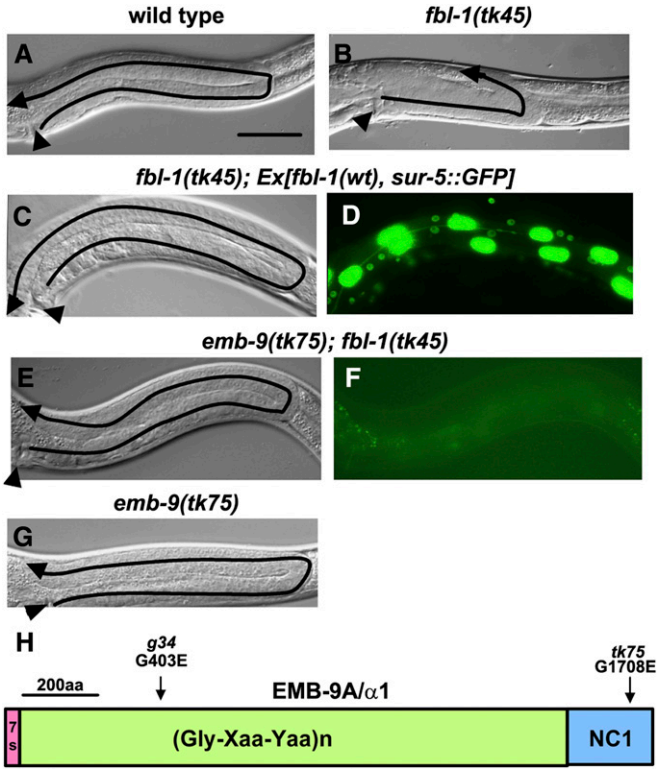

Figure 1 Gonadal phenotypes of the wild type and mutants. Nomarski (A–C, E, and G) and fluorescence (D and F) images of posterior gonads. Anterior is left, and dorsal is up. Posterior gonads of wild-type (A), *fbl-1(tk45)* (B), *fbl-1(tk45)*; *Ex[fbl-1(+), sur-5::GFP]* (C and D), *emb-9(tk75)*; *fbl-1(tk45)* (E and F), and *emb-9(tk75)* (G) hermaphrodites are shown. The predicted routes of DTC migration are shown by arrows. Arrowheads point to the vulvae. Bar, 50 μm. GFP is expressed in the somatic nuclei in D but not in F. (H) Domain structure of EMB-9 and the locations of mutations used in this study. Amino acid substitutions are shown. Amino acid positions in EMB-9 correspond to those of EMB-9A, one of the two alternatively spliced variants.

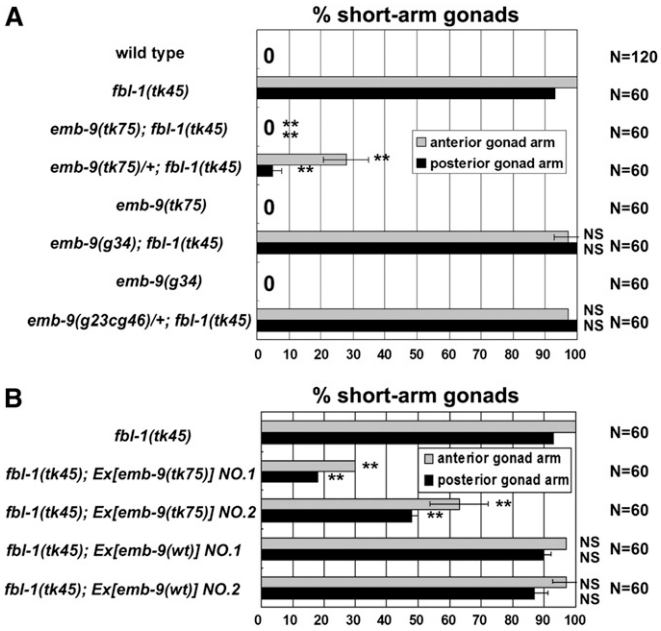

Figure 2 *emb-9(tk75)* suppresses the gonadal elongation defect of the *fbl-1(tk45)* mutant. (A) Quantification of gonadal elongation defects in *fbl-1* and *emb-9* mutants and in *emb-9*; *fbl-1* double mutants. Data are shown as the mean ± SD. Results for Fisher's exact test *vs. fbl-1(tk45)* are indicated; $^{**}P < 0.01$; NS, not significant. (B) Effects of mutant and wild-type (wt) *emb-9* transgenes on suppression. Two independent transgenic lines were examined for each transgene. The percentage of animals with anterior and posterior gonadal elongation defects is shown. Data are shown as the mean ± SD. Results for Fisher's exact test *vs. fbl-1(tk45)* are indicated; $^{**}P < 0.01$; NS, not significant.

Results

A dominant mutation in the type IV collagen α1 chain suppresses the gonadal defects in fbl-1(tk45) mutants

Fibulin family proteins are conserved ECM proteins (Argraves *et al.* 2003; Timpl *et al.* 2003). Loss-of-function mutations in *fbl-1* result in gonads with short and swollen arms (Figure 1, A and B) (Hesselson *et al.* 2004; Kubota *et al.* 2004; Muriel *et al.* 2005). We used EMS mutagenesis to isolate suppressors of *fbl-1(tk45)*, a null allele with a deletion in the *fbl-1* coding region (Kubota *et al.* 2004; Hesselson and Kimble 2006). Although *fbl-1(tk45)* homozygotes are sterile, a transgenic strain *fbl-1(tk45)*; *Ex[fbl-1(+), sur-5::GFP]* carrying an extrachromosomal array that consists of multiple copies of wild-type *fbl-1* and *sur-5::GFP* can proliferate as a homozygote (Kubota *et al.* 2004). *sur-5::GFP* is a marker construct that expresses GFP in all somatic nuclei. In this strain, 37% of F_1 animals ($n = 142$) inherited the GFP^+ extrachromosomal array and showed wild-type *U*-shaped gonad arm morphology (Figure 1, C and D). We isolated GFP^- animals with *U*-shaped gonad arms from the F_2 or F_3 generation of transgenic animals treated with EMS. Two independently isolated suppressor mutations, *tk75* and *tk76*, were found to be identical mutations in *emb-9*, which encodes the α1 subunit of type IV collagen (Guo *et al.* 1991). The mutation was a G-to-A transition, resulting in a change from Gly-1708 to Glu in the C-terminal noncollagenous 1 (NC1) domain of EMB-9A (Figure 1H, Supporting Information, Figure S1). *tk75* was dominant and strongly suppressed the short and swollen arm phenotype of *fbl-1(tk45)* mutants (Figures 1, E and F and 2A). The germ cells break out of the gonad and spread into the body cavity in older *fbl-1(tk45)* adults (Kubota *et al.* 2004). This phenotype was also suppressed by *tk75* (Figure S2).

Conventional *emb-9* mutations are embryonic or larval lethal (Gupta *et al.* 1997). In contrast, *tk75*, the suppressor of the *fbl-1* mutation, was homozygous viable and had no gonadal defects at 20° (Figures 1G and 2A). Only a small proportion of *tk75* animals exhibited short and swollen arm defects at 25° (11% of anterior gonad arms, 5% of posterior gonad arms; $n = 60$). We also investigated the effects of a known *emb-9* mutation on gonad morphogenesis in *fbl-1(tk45)* mutants. A temperature-sensitive (ts) embryonic lethal allele of *emb-9*, *g34* (Gupta *et al.* 1997), did not exhibit gonadal elongation defects at 20°, an intermediate temperature that results in growth retardation: 50% of *g34* larvae and 100% of wild-type larvae shifted from 16° to 20° at the

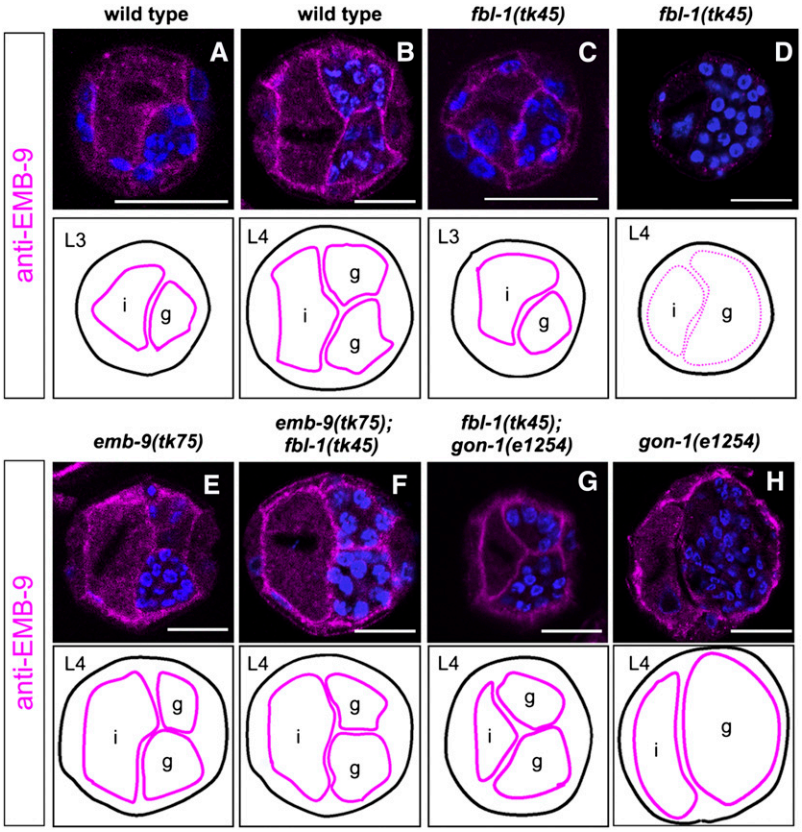

Figure 3 *emb-9(tk75)* and *gon-1(e1254)* suppress the reduced gonadal BM localization of EMB-9 in *fbl-1(tk45)* mutants. Localization of wild-type EMB-9 in wild type (A and B) and in the mutants *fbl-1(tk45)* (C and D), *fbl-1 (tk45); gon-1(e1254)* (G), and *gon-1(e1254)* (H). Localization of mutant EMB-9 in *emb-9(tk75)* (E) and *emb-9(tk75); fbl-1(tk45)* (F) animals. Cross-sections of L3 (A and C) and L4 (B and D–H) hermaphrodites were stained with anti–EMB-9 (magenta) and DAPI (blue) and analyzed with confocal microscopy. Borders of gonads and intestines are illustrated below the photos. Patterns of EMB-9 localization to the basement membrane are indicated by thick (normal) and dotted (weak and discontinuous) magenta lines. We observed similar results in more than three experimental sets (30–40 sections were observed for each genotype in an experiment). Bars, 25 μm. i, intestine; g, gonad.

first larval stage (L1) grew to be adults after 48 hr (n = 80). Shifting mutant L2 larvae to 25°, a restrictive temperature, resulted in severe gonadal defects (100% of both anterior and posterior gonad arms; n = 20) as reported (Kawano *et al.* 2009). *g34* could not suppress the *fbl-1(tk45)* mutants at 20° (Figure 2A). Because of the dominant suppression effect, we investigated whether *tk75* is a loss-of-function or a gain-of-function mutation. *emb-9(g23cg46)* (null)/+ exhibited no suppression activity. In addition, although the extrachromosomal transgenic arrays containing multiple wild-type copies of *emb-9* failed to suppress *fbl-1(tk45)*, the *emb-9(tk75)* mutant arrays significantly suppressed *fbl-1* defects (Figure 2B).These results suggest that *tk75* is a gain-of-function allele of *emb-9* that suppresses *fbl-1(tk45)*.

The suppressor EMB-9(tk75) localizes to BMs and suppresses loss of NID-1 from BMs in late larvae of fbl-1(tk45) mutants

EMB-9 is secreted from the body wall muscle cells and localizes to the BM (Graham *et al.* 1997). An antibody against EMB-9 clearly stained gonadal and intestinal BMs in wild-type hermaphrodites at the third and fourth larval stages (L3 and L4, respectively) (Figure 3, A and B). EMB-9 accumulation in *fbl-1(tk45)* mutants was normal at L3 but was markedly reduced and punctate at L4 (Figure 3, C and D). These results suggest that FBL-1 is not required for gonadal accumulation of EMB-9 prior to L4, but for maintaining EMB-9 localization in the gonadal BM during the late larval stages.

We next examined the localization of the suppressor EMB-9(*tk75*). Interestingly, the EMB-9(*tk75*) mutant protein was not lost from the gonadal and intestinal BMs in either *emb-9(tk75)* or *emb-9(tk75); fbl-1(tk45)* mutants at L4 (Figure 3, E and F). These results suggest that EMB-9 (*tk75*) suppresses the gonadal elongation defects of *fbl-1 (tk45)* by remaining localized to the gonadal BM during the late larval development.

We previously showed that *fbl-1* is required for BM localization of NID-1/nidogen, although *nid-1* null mutants have little effect on gonadogenesis (Kubota *et al.* 2008). We examined whether defective localization of NID-1 is suppressed by *emb-9(tk75)*. Anti–NID-1 detected a signal in the BM of the wild-type and *fbl-1(tk45)* L3 larvae, but the signal was substantially reduced in *fbl-1(tk45)* L4 larvae (Figure 4, A–D). As expected, the defective localization of NID-1 was suppressed by *emb-9(tk75)* (Figure 4, E and F), suggesting that the mutant EMB-9(*tk75*) protein acts to retain NID-1 in the BM in the late *fbl-1(tk45)* larvae.

emb-9(tk75) suppresses the reduced PAT-3 expression in fbl-1(tk45) mutants

Because integrins are major receptors for ECM proteins, we examined the expression of PAT-3–GFP (Plenefisch *et al.* 2000), a functional GFP fusion of β-integrin, in the DTCs. The expression of PAT-3–GFP in *fbl-1(tk45)* was significantly weaker than that in the wild type (Figure 5, A, B, and G). PAT-3–GFP was expressed normally in *emb-9(tk75)* mutants (Figure 5C). The expression of PAT-3–GFP reduced in *fbl-1*

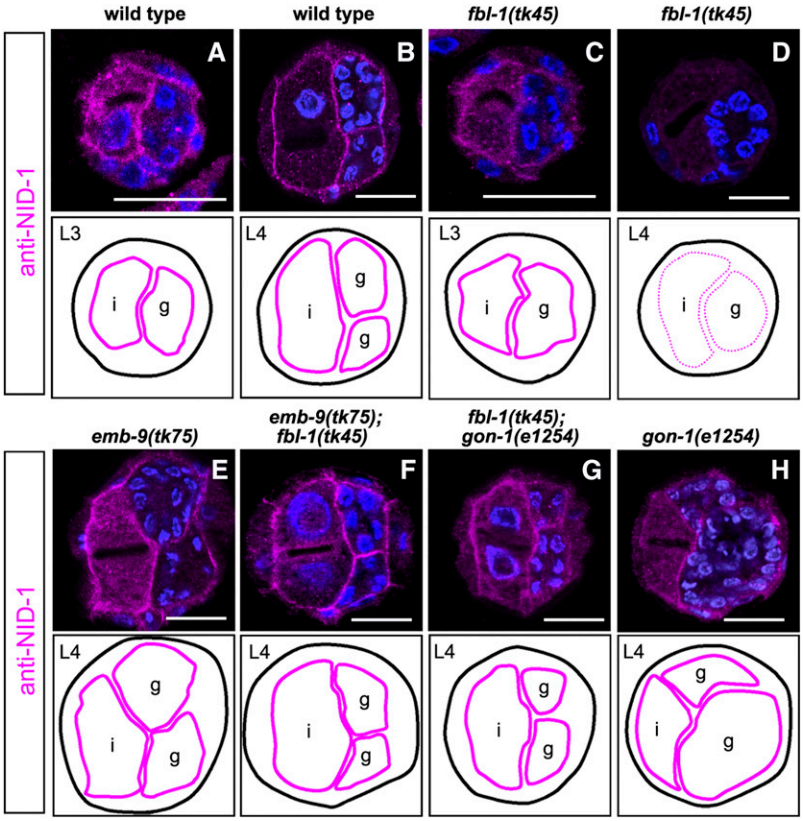

Figure 4 *emb-9(tk75)* and *gon-1(e1254)* suppress the reduced gonadal BM localization of NID-1 in *fbl-1(tk45)* mutants. Localization of wild-type NID-1 in wild type (A and B) and in the mutants *fbl-1(tk45)* (C and D), *fbl-1(tk45); gon-1(e1254)* (G), and *gon-1(e1254)* (H). Localization of mutant NID-1 in *emb-9(tk75)* (E) and *emb-9(tk75); fbl-1(tk45)* (F) animals. Cross-sections of L3 (A and C) and L4 (B and D–H) hermaphrodites were stained with anti–NID-1 (magenta) and DAPI (blue) and analyzed with confocal microscopy. Borders of gonads and intestines are illustrated below the photos. Patterns of NID-1 localization in the BM are indicated by thick (normal) and dotted (weak and discontinuous) magenta lines. We observed similar results in more than three experimental sets as in Figure 3. Bars, 25 μm. i, intestine; g, gonad.

(tk45) was restored in *emb-9(tk75); fbl-1(tk45)* double mutants (Figure 5, D, E, and G), indicating that *emb-9(tk75)* suppresses this phenotype of *fbl-1(tk45)*. PAT-3–GFP expression in *fbl-1(tk45)* was reduced in gonadal sheath cells in addition to DTCs, and this reduction was also suppressed by *emb-9(tk75)* (Figure S3). Similarly, DTC expression of INA-1–GFP, a functional GFP fusion of α-integrin, was reduced in *fbl-1(tk45)*, but it was restored in *emb-9(tk75); fbl-1(tk45)* animals (Figure S4).

Because EMB-9 localization was reduced in *fbl-1(tk45)* animals, it is possible that the reduction of EMB-9 in the BM causes the decrease of PAT-3 in DTCs. Therefore, we analyzed PAT-3–GFP expression in wild-type and *emb-9(g34)* animals reared at 25°, a nonpermissive temperature for *g34*. The EMB-9(*g34*) mutant protein accumulates in the cytoplasm and is not secreted at nonpermissive temperatures (Gupta *et al.* 1997). We observed that PAT-3–GFP expression was significantly reduced in the DTCs of *emb-9(g34)* mutants (Figure 5, F and H), suggesting that EMB-9/type IV collagen localization in the BM is important for proper PAT-3 expression. Finally, we examined whether overexpression of PAT-3 can rescue the DTC migration defects of *fbl-1* mutants. We found that PAT-3–GFP expression partially but significantly rescued the defects in *fbl-1* mutants (Figure 5I), indicating that reduction of PAT-3 expression contributes to the migration defects of DTCs in the *fbl-1* mutants.

A gon-1(e1254) allele also suppresses fbl-1(tk45)

Because an in-frame deletion mutation, *fbl-1(q750)* (a potential partial loss-of-function mutation) and a *gon-1(q518)* null mutation partially suppress the gonadal elongation defects resulting from each mutation, it has been proposed that wild-type FBL-1 and GON-1 have antagonistic roles in the control of gonadogenesis (Hesselson *et al.* 2004). Using the *gon-1* weak allele *e1254* (Blelloch *et al.* 1999; Blelloch and Kimble 1999), we investigated whether the combination of *fbl-1(tk45)* and *gon-1(e1254)* exhibits a similar genetic interaction. Although the suppression was partial, the gonadal phenotype of *fbl-1(tk45); gon-1(e1254)* double mutants was significantly weaker than that in either *fbl-1(tk45)* or *gon-1(e1254)* single mutants (Figure 6), indicating that they suppressed each other. EMB-9 and NID-1 accumulation decreased in *fbl-1(tk45)* L4 larvae (Figures 3D and 4D), but not *gon-1(e1254)* L4 larvae (Figures 3H and 4H). The reduced EMB-9 and NID-1 accumulation in *fbl-1(tk45)* animals was suppressed by *gon-1(e1254)* (Figures 3G and 4G). The reduced PAT-3-GFP expression in DTCs in *fbl-1(tk45)* animals was also suppressed by *gon-1(e1254)* (Figure 5, E and G).

emb-9(tk75) enhances the gonadal elongation defects in gon-1(e1254) mutants

We tested the genetic interaction between *emb-9* and *gon-1*. We used the *gon-1* weak allele *e1254* and null allele *q518* (Blelloch *et al.* 1999; Blelloch and Kimble 1999). The *emb-9(tk75); gon-1(e1254)* double mutants showed strong gonad morphogenesis defects similar to those observed in either *gon-1(q518)* or *emb-9(tk75); gon-1(q518)* mutants (Figure 7, A–E). *emb-9(tk75)/+* enhanced the gonadogenesis defects

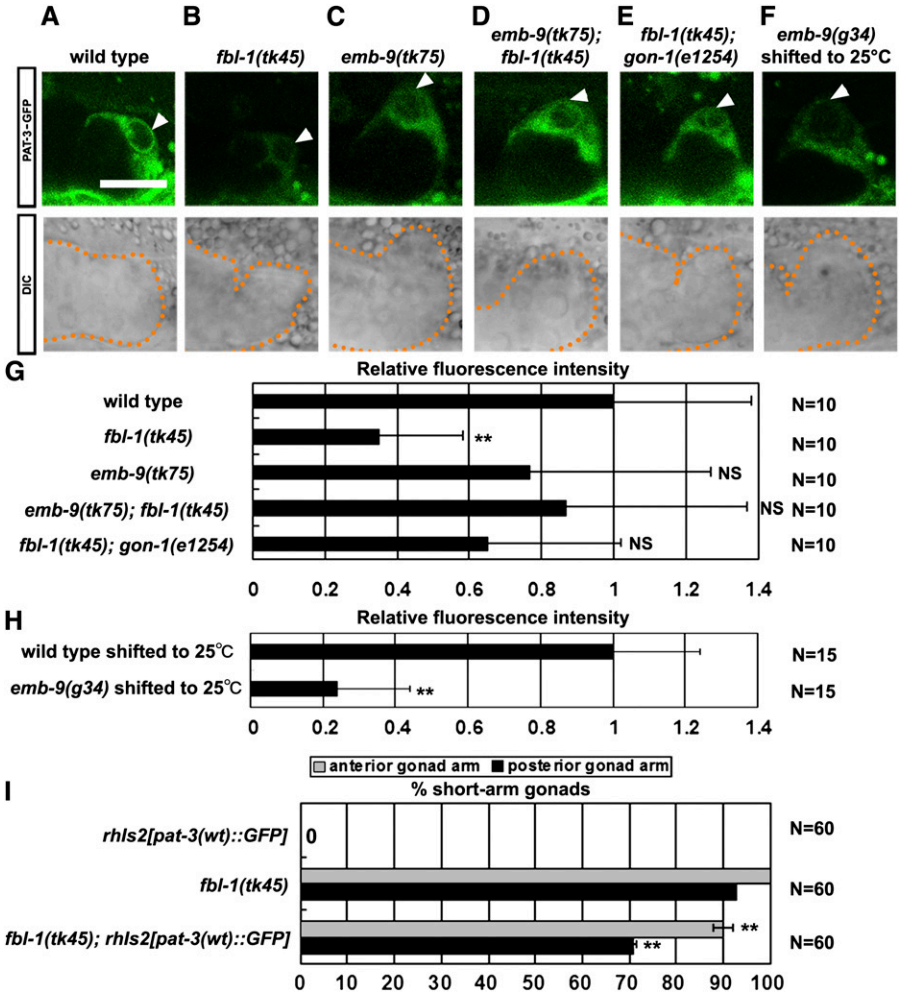

Figure 5 PAT-3–GFP localization in DTCs. Confocal (upper) and Nomarski (lower) images of wild-type (A), *fbl-1(tk45)* (B), *emb-9(tk75)* (C), *emb-9(tk75)*; *fbl-1(tk45)* (D), *fbl-1(tk45)*; *gon-1 (e1254)* (E), and *emb-9(g34)* (F) L3 hermaphrodites that expressed PAT-3–GFP. (F) *emb-9(g34)* mutants grown at 16° were shifted to 25° at the L2 larval stage. The arrowhead indicates PAT-3–GFP expression in DTCs. Scale bar, 20 μm. (G) Fluorescence intensity of PAT-3–GFP. All strains contained *rhIs2[pat-3(wt)::GFP]* in their background. The fluorescence intensity for each sample was normalized to that of the wild type. Ten confocal images of DTCs for each strain were used for quantification. The fluorescence intensity of a rectangular region (2.4 μm × 1.2 μm) at the tip of each DTC was quantified using the ImageJ program (National Institutes of Health), and values were averaged. Data are shown as the mean ± SD. Results for the Student's *t*-test *vs.* the wild-type value are indicated; $^{**}P < 0.01$; NS, not significant. All images were captured under the same conditions. (H) Fluorescence intensity of PAT-3–GFP in animals shifted to 25°. Fifteen animals for each strain were analyzed. The relative fluorescence intensity was determined as in G. (I) Effect of PAT-3–GFP overexpression in *fbl-1 (tk45)* mutants as analyzed by quantification of gonadal elongation defects. Data are shown as the mean ± SD. Results for Fisher's exact test *vs. fbl-1(tk45)* are indicated; $^{**}P < 0.01$.

of the *gon-1(e1254)* mutant (Figure 7E). The *emb-9(tk75)*; *gon-1(e1254)*; *fbl-1(tk45)* triple mutants exhibited intermediate phenotypes between those of *emb-9(tk75)*; *fbl-1(tk45)* and *gon-1(e1254)*; *fbl-1(tk45)* double mutants (Figure S5). Because *emb-9(tk75)* was a dominant enhancer of *gon-1 (e1254)*, we examined whether it is a gain-of-function or a loss-of-function mutation. Interestingly, we found that *emb-9(g23cg46)/+* enhanced the gonadal elongation defect of *gon-1(e1254)* mutants (Figure 7E), as was the case for *emb-9(tk75)/+*, suggesting that *emb-9(tk75)* acts as a loss-of-function mutation to enhance *gon-1(e1254)*. This is supported by the fact that the ts loss-of-function allele *emb-9 (g34)* enhanced the gonadal defects in *gon-1(e1254)* at 20° (Figure 7E). When we introduced multicopy mutant *emb-9 (tk75)* arrays into *gon-1(e1254)* mutants, the gonadal elongation defects were significantly enhanced, although wild-type *emb-9* arrays had no influence (Figure 7F). This could be because the wild-type EMB-9 was partially replaced by the overproduced mutant EMB-9(*tk75*) in the BM. The wild-type *fbl-1* arrays also significantly enhanced the gonadal elongation defects of *gon-1(e1254)* mutants (Figure 7F). Taken together, these results suggest that EMB-9(*tk75*) may have gained a FBL-1–like activity to inhibit the GON-1 function that is required for elongation and expansion of the gonad arms. Alternatively, wild type EMB-9 may act in parallel with GON-1.

Discussion

EMB-9(tk75) may affect interactions between NC1 domains

EMB-9/type IV collagen α1 subunit is secreted from muscle cells and DTCs, probably as a trimer (two α1 and one α2

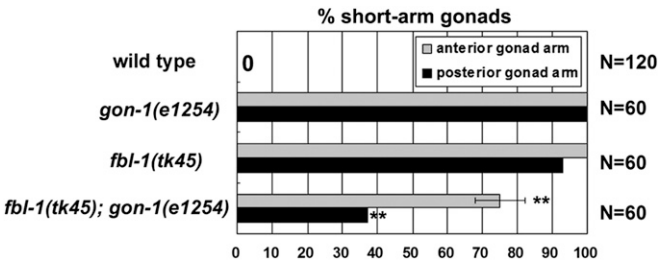

Figure 6 *fbl-1(tk45)* and *gon-1(e1254)* suppress each other with respect to the gonadal elongation defect. Quantification of gonadal elongation defects in *gon-1(e1254)*, *fbl-1(tk45)* and the double mutants. Data are shown as the mean ± SD. Result for Fisher's exact test *vs. fbl-1(tk45)* is indicated; $^{**}P < 0.01$.

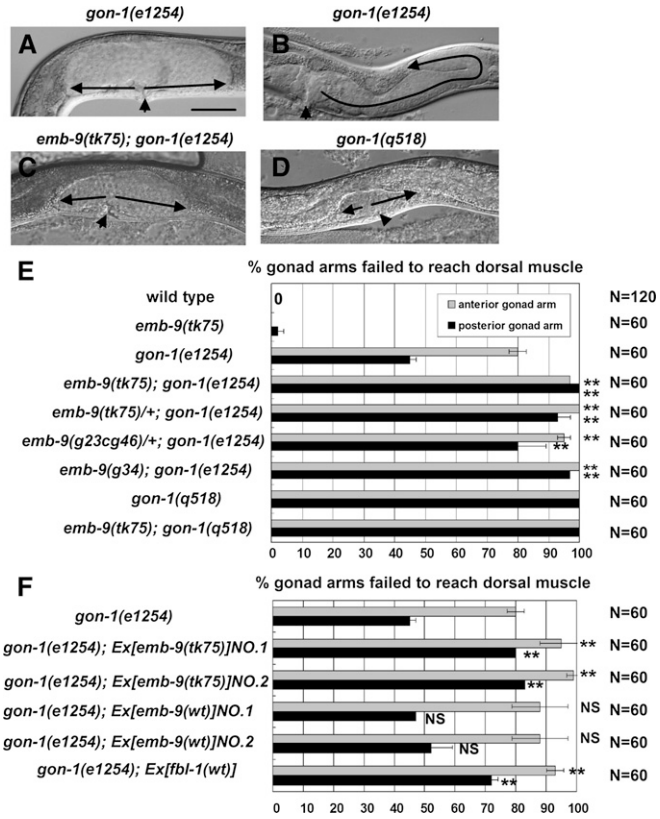

Figure 7 Genetic interaction between *emb-9* and *gon-1*. Phenotypes of posterior gonads of *gon-1(e1254)* (A and B), *emb-9 (tk75)*; *gon-1(e1254)* (C), and *gon-1(q518)* (D) hermaphrodites. Arrows and arrowheads are as in Figure 1. DTCs of posterior gonads in *emb-9(tk75)*; *gon-1(e1254)* and *gon-1(q518)* animals were often arrested during migration on the ventral muscle. Most *emb-9(tk75)*; *gon-1(e1254)* and *gon-1(q518)* mutants showed weak or no expansion of gonads. Bar, 50 μm. (E) Quantification of gonad arms that failed to reach the dorsal muscle. Data are shown as the mean ± SD. Results for Fisher's exact test *vs. gon-1(e1254)* are indicated; $^{**}P < 0.01$; NS, not significant. (F) Effects of extrachromosomal arrays containing mutant *emb-9*, wild-type (wt) *emb-9*, and wild-type *fbl-1* transgenes. Quantification of gonad arms that failed to reach the dorsal muscle. Data are shown as the mean ± SD. Results for Fisher's exact test *vs. gon-1(e1254)* are indicated; $^{**}P < 0.01$; NS, not significant.

subunits) together with LET-2/type IV collagen α2 subunit and accumulates in the BM (Gupta *et al.* 1997). Unlike *emb-9 (g34)* animals, which fail to secrete type IV collagen at nonpermissive temperatures (Gupta *et al.* 1997), *emb-9(tk75)*; *fbl-1(tk45)* mutants exhibited mostly normal type IV collagen secretion, and the collagen clearly localized to the gonadal BM, implying that the strong suppression is probably due to a defect in the BM, which is induced by secreted mutant EMB-9(*tk75*). Gly-1708, which is substituted in the *tk75* mutation, is evolutionarily conserved and is a component of the trimer–trimer interface region. This region is important for interactions between individual NC1 domains of collagen subunit trimers, which form the type IV collagen network (Figure S1) (Sundaramoorthy *et al.* 2002). Because the *tk75* mutants are viable and fertile, the gonadal BM is presumably not as seriously impaired as in the lethal *emb-9* or *let-2* mutants (Gupta *et al.* 1997). The marked reduction of type IV collagen

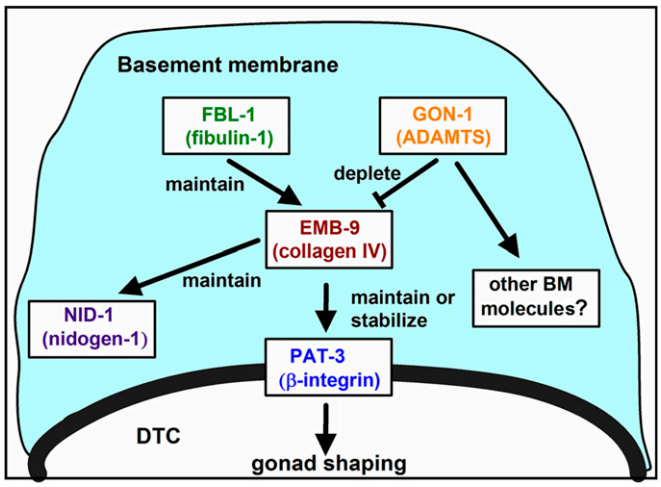

Figure 8 A model of the interactions among FBL-1, EMB-9, and GON-1 in gonad shaping. In the late larval stages, FBL-1 acts to maintain EMB-9, whereas GON-1 depletes EMB-9 to achieve appropriate levels of EMB-9 localization in the BM. The BM-localized EMB-9 maintains NID-1 in the BM and promotes expression or stabilization of PAT-3 in DTCs (and gonadal sheath cells). GON-1 may also affect other BM molecules.

localization in the swollen gonad arms of *fbl-1(tk45)* mutants during late larval stages suggests that stage-specific maintenance of the type IV collagen network is required to generate gonads of the proper length and width. One possibility is that the trimer–trimer interactions between EMB-9(*tk75*) molecules may be strengthened during the late larval stages so that this protein is not lost from the BM in the absence of FBL-1. *emb-9(tk75)* also suppressed the defective maintenance of NID-1 in *fbl-1(tk45)* mutants, suggesting that EMB-9(*tk75*) acts to maintain NID-1. This is consistent with our previous observation that NID-1 localization is reduced in the ts *let-2(b246)* (α2 chain of type IV collagen) mutants reared at nonpermissive temperatures (Kubota *et al.* 2008). Because type IV collagen interacts with nidogen (Aumailley *et al.* 1989), it might be possible that EMB-9(*tk75*) acts as an anchor for NID-1.

Type IV collagen may be required for integrin-dependent gonadal elongation

Integrin family receptors consist of two subunits, α- and β-integrins. The regulated expression of two α-integrins, INA-1 and PAT-2, controls DTC migration; INA-1 is required for continuous migration, whereas PAT-2 is required for pathfinding in migration (Meighan and Schwarzbauer 2007). PAT-3 is the sole β-integrin in *C. elegans*. A dominant-negative PAT-3 disrupts DTC migration (Lee *et al.* 2001). We found that the expression of PAT-3–GFP in DTCs, as well as the BM localization of EMB-9, was reduced in *fbl-1(tk45)* mutants. A similar reduction in PAT-3–GFP expression was also observed in the *emb-9(g34)* ts mutant, in which the mutant EMB-9 (*g34*) fails to be secreted. These results suggest that EMB-9 accumulation in the BM upregulates the expression of PAT-3 or stabilizes PAT-3 in DTCs. Consistent with this idea, the PAT-3–GFP reduction in *fbl-1(tk45)* mutants was suppressed

in both *emb-9(tk75)*; *fbl-1(tk45)* and *fbl-1(tk45)*; *gon-1 (e1254)* double mutants, in which EMB-9 accumulation was restored. A correlation between type IV collagen and the integrin expression level has been observed in pancreatic β cells. Type IV collagen promotes the α1β1 integrin-dependent migration on Matrigel of β cells in which integrin expression is upregulated (Kaido *et al.* 2004). Because integrins are major receptors for ECM proteins and regulate cytoskeletal activity (Bokel and Brown 2002; Wiesner *et al.* 2005; Berrier and Yamada 2007), accumulation of type IV collagen in BMs probably plays an important role in integrin-dependent cytoskeletal regulation. We observed that overexpression of PAT-3–GFP can partly suppress *fbl-1* mutants. Thus, it is possible that EMB-9 may mediate FBL-1 function to promote integrin expression and cytoskeletal rearrangement in DTCs, which are required for gonadal elongation. In support of this, RNAi knockdown of *ina-1* and ts *let-2* and *emb-9* mutants reared at nonpermissive temperatures exhibit the short-arm gonad phenotype (Cram *et al.* 2006; Meighan and Schwarzbauer 2007; Kawano *et al.* 2009) similar to that observed in *fbl-1(tk45)* mutants.

A similar reduction in PAT-3–GFP expression in *fbl-1(tk45)* animals and the resumption of its expression in *emb-9(tk75)*; *fbl-1(tk45)* animals were observed in gonadal sheath cells, suggesting that type IV collagen regulation of β-integrin also occurs in sheath cells. The sheath cells modulate gonad morphogenesis by activating integrin signaling (Baum and Garriga 1997; Lee *et al.* 2005).

Interactions among FBL-1, EMB-9, and GON-1 in the regulation of gonadogenesis

Because the *fbl-1(tk45)* null mutation is suppressed almost completely by *emb-9(tk75)*, it is possible that the major function of FBL-1 is to maintain EMB-9, which leads to BM accumulation of NID-1 and expression of PAT-3 in the somatic gonad (Figure 8). Although its suppression is weaker than that of *emb-9(tk75)*, *gon-1(e1254)* shares similar suppression characteristics with *emb-9(tk75)*. Thus, it is possible that GON-1 interacts with the FBL-1 pathway. We speculate that EMB-9 may be located downstream of and regulated negatively by GON-1 (Figure 8). In this model, we postulated that the amount of BM-localized EMB-9 is maintained appropriately by a balance between EMB-9 accumulation (regulated by FBL-1) and its reduction by GON-1. This model can explain the dominant enhancing effect of EMB-9(*tk75*) if this mutation leads to its inappropriate maintenance in the BM despite the action of GON-1(*e1254*), which could have a much weaker effect than that of wild-type GON-1. This hypothesis does, however, raise a question as to why *emb-9(g23cg46)/+* enhances *gon-1(e1254)*. We speculate that reduction of GON-1 activity in *gon-1(e1254)* animals affects several BM proteins, including EMB-9, by modifying the localization or conformation of these proteins in the BM. When *gon-1(e1254)* is combined with *emb-9(g23cg46)/+*, which should disrupt the EMB-9–LET-2 stoichiometry in type IV collagen, this may further degrade the general physiology of the BM, resulting in phenotypic enhancement of *gon-1(e1254)*. We could not determine whether EMB-9 localization was upregulated in the *gon-1* mutants, because the immunohistochemical experiments performed in this study were not sensitive enough to assess subtle differences in protein localization. Further studies will be required to determine the precise mechanism of suppression underlying the action of EMB-9(*tk75*) and GON-1(*e1254*).

The *C. elegans* gonad is a tubular structure that is covered with a BM (Hall *et al.* 1999). Type IV collagen is a major component of the BM and associates with other ECM molecules such as laminin, nidogen, and heparan sulfate proteoglycans in mammals (Fujiwara *et al.* 1984; Charonis *et al.* 1985; Aumailley *et al.* 1989). Mouse type IV collagen also interacts weakly with fibulin-1 *in vitro* (Pan *et al.* 1993). Therefore, EMB-9 and FBL-1 may bind directly or indirectly through other ECM molecules to form a supramolecular network in the BM to regulate gonadogenesis. Similar to the stage-specific function of FBL-1 in *C. elegans*, mouse fibulin-1 is required for maintenance of integrity of small vessels only after midgestation (Kostka *et al.* 2001), suggesting that fibulin-1 may have a conserved role in temporal regulation of structure and function of the BM. GON-1, which is homologous to mammalian ADAMTS-9 and ADAMTS-20 proteinases (Llamazares *et al.* 2003; Somerville *et al.* 2003), may act to degrade EMB-9. The interactions among these molecules probably affect the balance between gonadal elongation and expansion activities. Our findings provide the functional evidence for interactions among conserved molecules fibulin-1, type IV collagen, and an ADAMTS and therefore suggest an interesting possibility that a similar functional interaction may also occur in mammalian organogenesis.

Acknowledgments

We thank Jim Kramer for type IV collagen antibodies, John Plenefisch for a strain with an *rhIs2* insertion, Alan Coulson for cosmid clones, and the *Caenorhabditis* Genetics Center for strains. We also thank Noriko Nakagawa and Asami Sumitani for technical assistance. We thank Masaki Kakehi for sharing unpublished results. This work was supported by a grant-in-aid for scientific research by the Ministry of Education, Culture, Sports, Science, and Technology to Y.K. (18570213) and Natural Science Scholarship by the Naito Foundation to K.N.

Literature Cited

Argraves, W. S., L. M. Greene, M. A. Cooley, and W. M. Gallagher, 2003 Fibulins: physiological and disease perspectives. EMBO Rep. 4: 1127–1131.

Aumailley, M., H. Wiedemann, K. Mann, and R. Timpl, 1989 Binding of nidogen and the laminin-nidogen complex to basement membrane collagen type IV. Eur. J. Biochem. 184: 241–248.

Baum, P. D., and G. Garriga, 1997 Neuronal migrations and axon fasciculation are disrupted in *ina-1* integrin mutants. Neuron 19: 51–62.

Berrier, A. L., and K. M. Yamada, 2007 Cell-matrix adhesion. J. Cell. Physiol. 213: 565–573.

Bianco, A., M. Poukkula, A. Cliffe, J. Mathieu, C. M. Luque *et al.*, 2007 Two distinct modes of guidance signalling during collective migration of border cells. Nature 448: 362–365.

Blelloch, R., and J. Kimble, 1999 Control of organ shape by a secreted metalloprotease in the nematode *Caenorhabditis elegans*. Nature 399: 586–590.

Blelloch, R., S. S. Anna-Arriola, D. Gao, Y. Li, J. Hodgkin *et al.*, 1999 The *gon-1* gene is required for gonadal morphogenesis in *Caenorhabditis elegans*. Dev. Biol. 216: 382–393.

Bokel, C., and N. H. Brown, 2002 Integrins in development: moving on, responding to, and sticking to the extracellular matrix. Dev. Cell 3: 311–321.

Brenner, S., 1974 The genetics of *Caenorhabditis elegans*. Genetics 77: 71–94.

Charonis, A. S., E. C. Tsilibary, P. D. Yurchenco, and H. Furthmayr, 1985 Binding of laminin to type IV collagen: a morphological study. J. Cell Biol. 100: 1848–1853.

Cram, E. J., H. Shang, and J. E. Schwarzbauer, 2006 A systematic RNA interference screen reveals a cell migration gene network in *C. elegans*. J. Cell Sci. 119: 4811–4818.

Ewald, A. J., A. Brenot, M. Duong, B. S. Chan, and Z. Werb, 2008 Collective epithelial migration and cell rearrangements drive mammary branching morphogenesis. Dev. Cell 14: 570–581.

Friedl, P., and D. Gilmour, 2009 Collective cell migration in morphogenesis, regeneration and cancer. Nat. Rev. Mol. Cell Biol. 10: 445–457.

Fujiwara, S., H. Wiedemann, R. Timpl, A. Lustig, and J. Engel, 1984 Structure and interactions of heparan sulfate proteoglycans from a mouse tumor basement membrane. Eur. J. Biochem. 143: 145–157.

Graham, P. L., J. J. Johnson, S. Wang, M. H. Sibley, M. C. Gupta *et al.*, 1997 Type IV collagen is detectable in most, but not all, basement membranes of *Caenorhabditis elegans* and assembles on tissues that do not express it. J. Cell Biol. 137: 1171–1183.

Guo, X. D., J. J. Johnson, and J. M. Kramer, 1991 Embryonic lethality caused by mutations in basement membrane collagen of *C. elegans*. Nature 349: 707–709.

Gupta, M. C., P. L. Graham, and J. M. Kramer, 1997 Characterization of α1(IV) collagen mutations in *Caenorhabditis elegans* and the effects of α1 and α2(IV) mutations on type IV collagen distribution. J. Cell Biol. 137: 1185–1196.

Hall, D. H., V. P. Winfrey, G. Blaeuer, L. H. Hoffman, T. Furuta *et al.*, 1999 Ultrastructural features of the adult hermaphrodite gonad of *Caenorhabditis elegans*: relations between the germ line and soma. Dev. Biol. 212: 101–123.

Hedgecock, E. M., J. G. Culotti, D. H. Hall, and B. D. Stern, 1987 Genetics of cell and axon migrations in *Caenorhabditis elegans*. Development 100: 365–382.

Hesselson, D., and J. Kimble, 2006 Growth control by EGF repeats of the *C. elegans* Fibulin-1C isoform. J. Cell Biol. 175: 217–223.

Hesselson, D., C. Newman, K. W. Kim, and J. Kimble, 2004 GON-1 and fibulin have antagonistic roles in control of organ shape. Curr. Biol. 14: 2005–2010.

Kaido, T., M. Yebra, V. Cirulli, and A. M. Montgomery, 2004 Regulation of human β-cell adhesion, motility, and insulin secretion by collagen IV and its receptor $\alpha_1\beta_1$. J. Biol. Chem. 279: 53762–53769.

Kawano, T., H. Zheng, D. C. Merz, Y. Kohara, K. K. Tamai *et al.*, 2009 *C. elegans mig-6* encodes papilin isoforms that affect distinct aspects of DTC migration, and interacts genetically with *mig-17* and collagen IV. Development 136: 1433–1442.

Kimble, J., and D. Hirsh, 1979 The postembryonic cell lineages of the hermaphrodite and male gonads in *Caenorhabditis elegans*. Dev. Biol. 70: 396–417.

Kostka, G., R. Giltay, W. Bloch, K. Addicks, R. Timpl *et al.*, 2001 Perinatal lethality and endothelial cell abnormalities in several vessel compartments of fibulin-1-deficient mice. Mol. Cell. Biol. 21: 7025–7034.

Kubota, Y., R. Kuroki, and K. Nishiwaki, 2004 A fibulin-1 homolog interacts with an ADAM protease that controls cell migration in *C. elegans*. Curr. Biol. 14: 2011–2018.

Kubota, Y., M. Sano, S. Goda, N. Suzuki, and K. Nishiwaki, 2006 The conserved oligomeric Golgi complex acts in organ morphogenesis via glycosylation of an ADAM protease in *C. elegans*. Development 133: 263–273.

Kubota, Y., K. Ohkura, K. K. Tamai, K. Nagata, and K. Nishiwaki, 2008 MIG-17/ADAMTS controls cell migration by recruiting nidogen to the basement membrane in *C. elegans*. Proc. Natl. Acad. Sci. USA 105: 20804–20809.

Lee, M., E. J. Cram, B. Shen, and J. E. Schwarzbauer, 2001 Roles for βpat-3 integrins in development and function of *Caenorhabditis elegans* muscles and gonads. J. Biol. Chem. 276: 36404–36410.

Lee, M., B. Shen, J. E. Schwarzbauer, J. Ahn, and J. Kwon, 2005 Connections between integrins and Rac GTPase pathways control gonad formation and function in *C. elegans*. Biochim. Biophys. Acta 1723: 248–255.

Llamazares, M., S. Cal, V. Quesada, and C. Lopez-Otin, 2003 Identification and characterization of ADAMTS-20 defines a novel subfamily of metalloproteinases-disintegrins with multiple thrombospondin-1 repeats and a unique GON domain. J. Biol. Chem. 278: 13382–13389.

Lu, P., and Z. Werb, 2008 Patterning mechanisms of branched organs. Science 322: 1506–1509.

Maduro, M., and D. Pilgrim, 1995 Identification and cloning of *unc-119*, a gene expressed in the *Caenorhabditis elegans* nervous system. Genetics 141: 977–988.

McCulloch, D. R., C. M. Nelson, L. J. Dixon, D. L. Silver, J. D. Wylie *et al.*, 2009 ADAMTS metalloproteases generate active versican fragments that regulate interdigital web regression. Dev. Cell 17: 687–698.

Meighan, C. M., and J. E. Schwarzbauer, 2007 Control of *C. elegans* hermaphrodite gonad size and shape by vab-3/Pax6-mediated regulation of integrin receptors. Genes Dev. 21: 1615–1620.

Mello, C. C., J. M. Kramer, D. Stinchcomb, and V. Ambros, 1991 Efficient gene transfer in *C. elegans*: extrachromosomal maintenance and integration of transforming sequences. EMBO J. 10: 3959–3970.

Miwa, J., E. Schierenberg, and S. Miwa, and G. von Ehrenstein, 1980 Genetics and mode of expression of temperature-sensitive mutations arresting embryonic development in *Caenorhabditis elegans*. Dev. Biol. 76: 160–174.

Montell, D. J., 2008 Morphogenetic cell movements: diversity from modular mechanical properties. Science 322: 1502–1505.

Muriel, J. M., C. Dong, H. Hutter, and B. E. Vogel, 2005 Fibulin-1C and Fibulin-1D splice variants have distinct functions and assemble in a hemicentin-dependent manner. Development 132: 4223–4234.

Nishiwaki, K., 1999 Mutations affecting symmetrical migration of distal tip cells in *Caenorhabditis elegans*. Genetics 152: 985–997.

Nishiwaki, K., N. Hisamoto, and K. Matsumoto, 2000 A metalloprotease disintegrin that controls cell migration in *Caenorhabditis elegans*. Science 288: 2205–2208.

Pan, T. C., M. Kluge, R. Z. Zhang, U. Mayer, R. Timpl *et al.*, 1993 Sequence of extracellular mouse protein BM-90/fibulin and its calcium-dependent binding to other basement-membrane ligands. Eur. J. Biochem. 215: 733–740.

Plenefisch, J. D., X. Zhu, and E. M. Hedgecock, 2000 Fragile skeletal muscle attachments in dystrophic mutants of *Caenorhabditis elegans*: isolation and characterization of the mua genes. Development 127: 1197–1207.

Rorth, P., 2009 Collective cell migration. Annu. Rev. Cell Dev. Biol. 25: 407–429.

Somerville, R. P., J. M. Longpre, K. A. Jungers, J. M. Engle, M. Ross *et al.*, 2003 Characterization of ADAMTS-9 and ADAMTS-20

as a distinct ADAMTS subfamily related to *Caenorhabditis elegans* GON-1. J. Biol. Chem. 278: 9503–9513.
Sundaramoorthy, M., M. Meiyappan, P. Todd, and B. G. Hudson, 2002 Crystal structure of NC1 domains. Structural basis for type IV collagen assembly in basement membranes. J. Biol. Chem. 277: 31142–31153.
Timpl, R., T. Sasaki, G. Kostka, and M. L. Chu, 2003 Fibulins: a versatile family of extracellular matrix proteins. Nat. Rev. Mol. Cell Biol. 4: 479–489.
Wicks, S. R., R. T. Yeh, W. R. Gish, R. H. Waterston, and R. H. Plasterk, 2001 Rapid gene mapping in *Caenorhabditis elegans* using a high density polymorphism map. Nat. Genet. 28: 160–164.
Wiesner, S., K. R. Legate, and R. Fassler, 2005 Integrin-actin interactions. Cell. Mol. Life Sci. 62: 1081–1099.
Yochem, J., T. Gu, and M. Han, 1998 A new marker for mosaic analysis in *Caenorhabditis elegans* indicates a fusion between hyp6 and hyp7, two major components of the hypodermis. Genetics 149: 1323–1334.

Communicating editor: D. I. Greenstein

GENETICS

Supporting Information
http://www.genetics.org/content/suppl/2012/01/31/genetics.111.133173.DC1

Tissue Architecture in the *Caenorhabditis elegans* Gonad Depends on Interactions Among Fibulin-1, Type IV Collagen and the ADAMTS Extracellular Protease

Yukihiko Kubota, Kayo Nagata, Asako Sugimoto, and Kiyoji Nishiwaki

DOI: 10.1534/genetics.111.133173

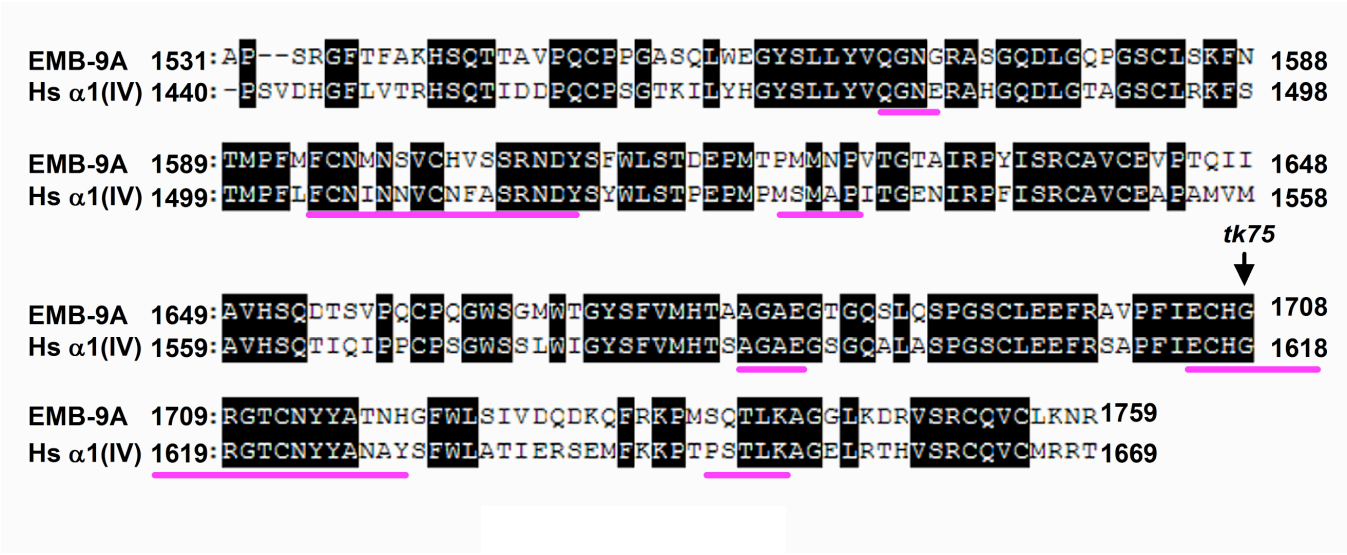

Figure S1 EMB-9(*tk75*) has a substitution at an evolutionarily conserved amino acid in the NC1 domain. Alignment of the C-terminal NC1 domain sequences of the type IV collagen α1 chains of *C. elegans* (EMB-9) and humans [Hs α1 (IV)]. The amino acids in the trimer-trimer interface region (Sundaramoorthy *et al.* 2002) are underlined in magenta. Identical amino acids are boxed (black). The mutated glycine in *tk75* is indicated.

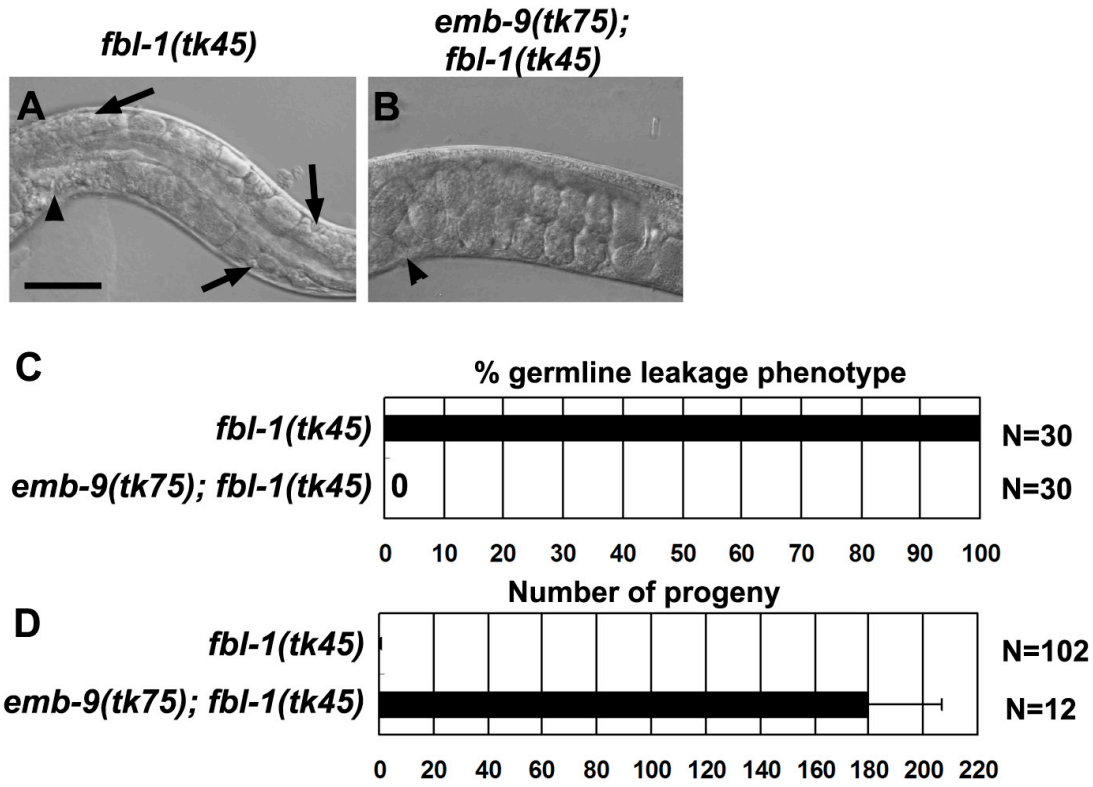

Figure S2 Germ line phenotype. (A) The germ cells (arrows) were released into the body cavity in 1-day-old *fbl-1(tk45)* adult hermaphrodites, probably because of the defects in the BM. (B) This phenotype was not observed in 1-day-old *emb-9(tk75); fbl-1(tk45)* adult hermaphrodites. Arrowheads point to the vulvae. Scale bar, 25 μm. Quantification of the germ line phenotype (C), n = 30. One-day-old adult hermaphrodites were scored for the presence of germ cells in the body cavity by Nomarski microscopy; Quantification of brood sizes (D), n = 102 for *fbl-1(tk45)* and n = 12 for *emb-9(tk75); fbl-1(tk45)*. Brood size is the number of hatched larvae from eggs laid by an adult hermaphrodite during 72 hours.

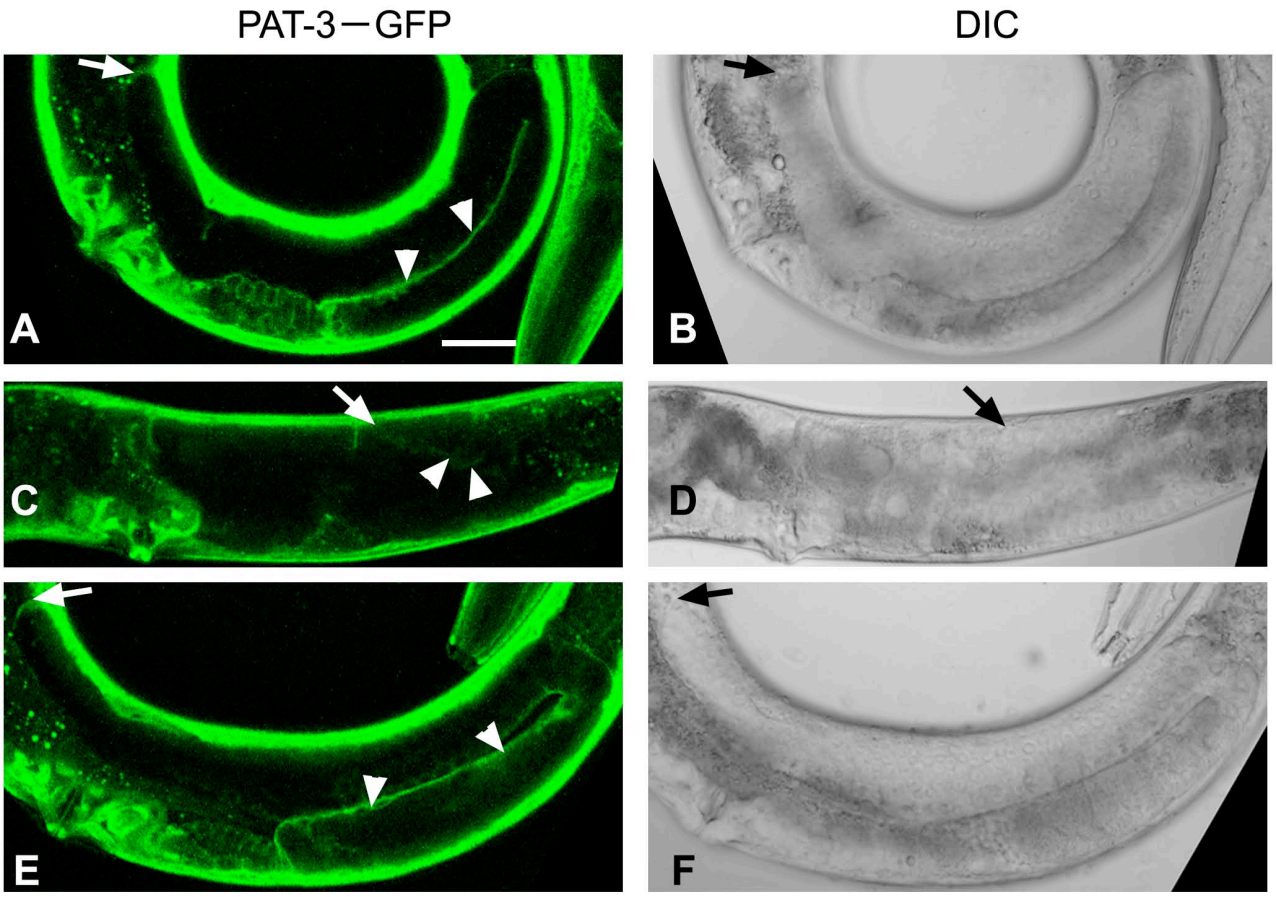

Figure S3 PAT-3-GFP expression in the gonadal sheath cells. Confocal (A, C, E) and Nomarski (B, D, F) images of posterior gonads of wild-type (A, B), *fbl-1(tk45)* (C, D), and *emb-9(tk75); fbl-1(tk45)* (E, F) young adult hermaphrodites expressing PAT-3-GFP. Arrows indicate PAT-3-GFP expression in DTCs. Arrowheads indicate PAT-3-GFP expression in gonadal sheath cells. The weakened PAT-3-GFP expression in DTCs and sheath cells in *fbl-1(tk45)* animals (C, D) recovered to wild-type levels in *emb-9(tk75); fbl-1(tk45)* animals (E, F). All images were captured under the same conditions. Scale bar, 25 μm.

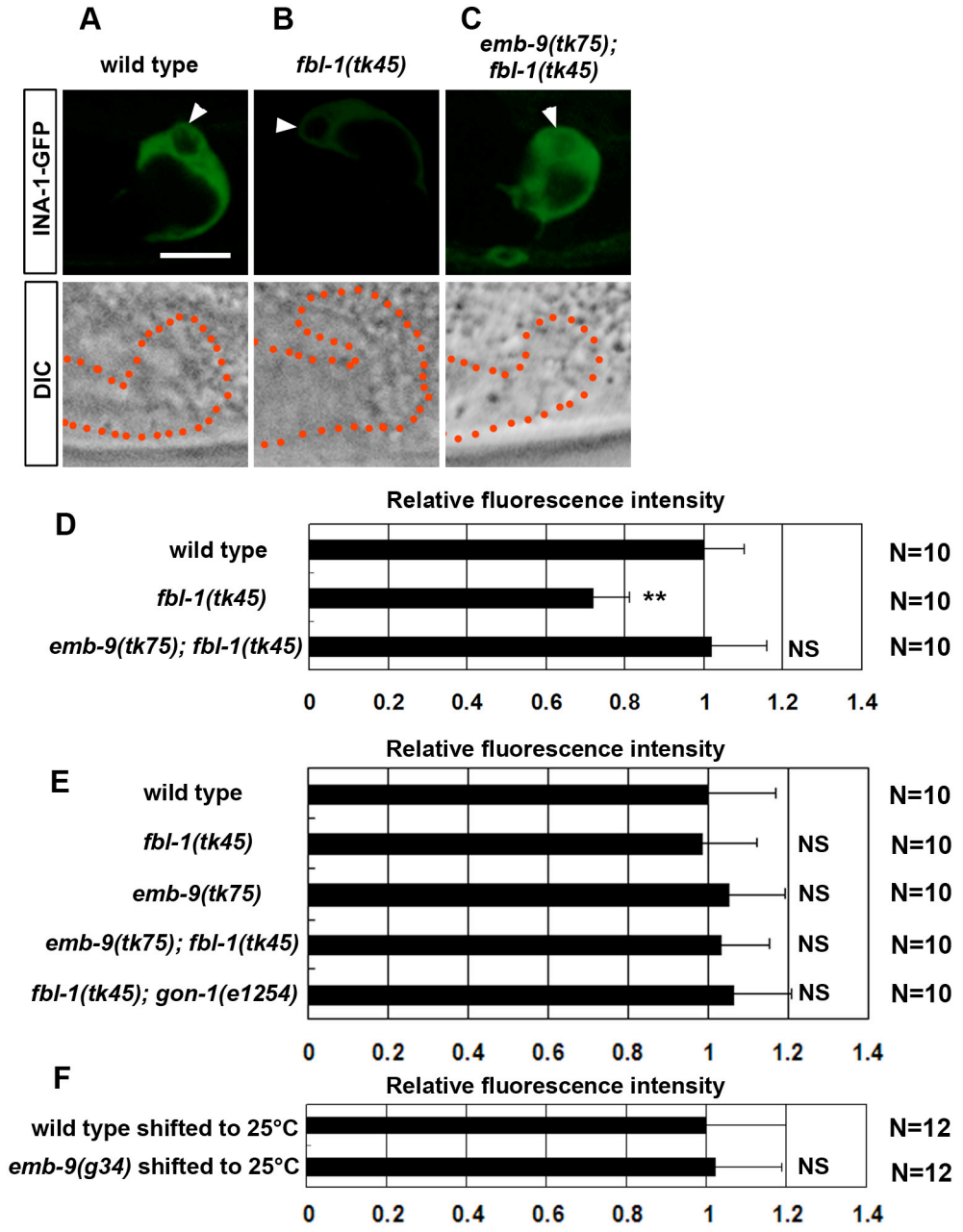

Figure S4 INA-1-GFP expression in DTCs**.** Images were captured by CSU-X1 spinning-disc conforcal system (Yokogawa Electric Corp.) mounted on Axioplan 2 microscope (Zeiss) equipped with a C-apochromat 63X (water immersion; NA 1.2) lens and controlled by MetaMorph software (Molecular Devices Inc.). (A, B, C) *ina-1::GFP* expression. Confocal (upper) and Nomarski (lower) images of L3 hermaphrodites of wild type (A), *fbl-1(tk45)* (B), *emb-9(tk75); fbl-1(tk45)* (C) having *gmIs5* that contain chromosomally integrated *ina-1::GFP* plasmids (Baum & Garriga 1997). The arrowhead indicates the INA-1-GFP expression in DTCs. Scale bar, 20 μm. (D) Fluorescence intensity of INA-1-GFP. The fluorescence intensity for each sample was normalized to that of the wild type. Ten confocal

images of DTCs for each strain were used for quantification. The relative fluorescence intensity was determined as in Figure 5G. Data are shown as the mean ± SD. Results for Student's *t*-test versus wild type are indicated; **, P<0.01; NS, not significant. All images were captured under the same conditions. (E, F) *lag-2p::GFP* expression. As a control, we examined *lag-2p::GFP* expression in DTCs and found that it is not affected by genetic backgrounds used in this work. All strains have *qIs56* that contains chromosomally integrated *lag-2p::GFP* plasmids (Blelloch *et al.* 1999) in their background. The fluorescence intensity for each sample was normalized to that of the wild type. Ten or twelve confocal images of DTCs for each strain were used for quantification. The relative fluorescence intensity was determined as in Figure 5G. Data are shown as the mean ± SD. Results for the Student's *t*-test against the wild-type value are indicated; NS, not significant. All images were captured under the same conditions.

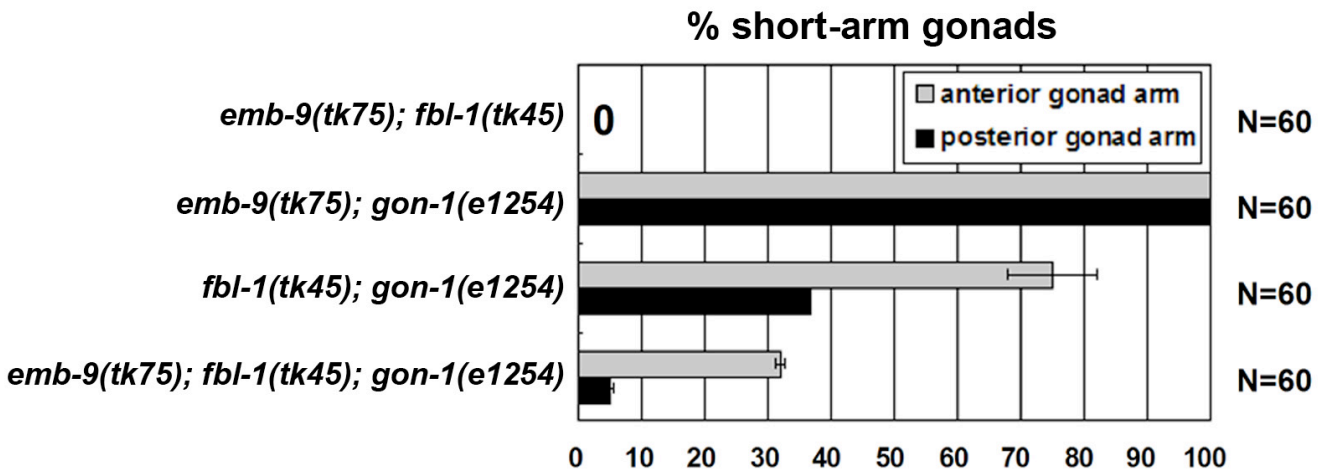

Figure S5 Gonadal elongation defects in the *emb-9(tk75); fbl-1(tk45)*; *gon-1(e1254)* triple mutants

Data for double mutants are included for comparison.

LITERATURE CITED

Baum, P. D., and G. Garriga, 1997 Neuronal migrations and axon fasciculation are disrupted in *ina-1* integrin mutants. Neuron **19**: 51-62.

Blelloch, R., S. S. Anna-Arriola, D. Gao, Y. Li, J. Hodgkin *et al.* 1999 The *gon-1* gene is required for gonadal morphogenesis in *Caenorhabditis elegans*. Dev.Biol. **216**: 382-393.

Sundaramoorthy, M., M. Meiyappan, P. Todd, and B. G. Hudson, 2002 Crystal structure of NC1 domains. Structural basis for type IV collagen assembly in basement membranes. J.Biol.Chem. **277**: 31142-31153.